SF2A 2014
J. Ballet, F. Bournaud, F. Martins, R. Monier and C. Reylé (eds)

HELIUM SIGNATURE IN RED GIANT OSCILLATION SPECTRA

Vrard M.[1], Mosser B.[1] and Barban C.[1]

Abstract. The space telescopes CoRoT and *Kepler* have provided seismic data of unprecedent quality on red giants. The oscillation spectrum of these stars have shown a regular pattern called the universal oscillation pattern. These very precise data allow us to study the deviation from this regular pattern. In this work, we measure the modulation component of the radial mode frequency spacing in more than one hundred red giants and attribute the modulation to glitches due to the region of second ionisation of helium. We find a correlation between the location of this zone and the evolutionary status of the red giants. These results brings new constraints on the star interiors.

Keywords: stars : pulsations, stars : evolution

1 Introduction

Solar-like oscillations have been detected in thousands of red giants, with the CoRoT and *Kepler* missions. The radial modes discovered in these stars spectrum are p-modes forming a regular pattern called universal red giant oscillation pattern (Mosser et al. 2011). Because of sound speed discontinuities, departures from this universal pattern are observed. The aim of this work is to study these deviations called glitches which are produced by inner structure discontinuities of the star, such as the base of the convection zone or the second helium ionisation zone (Gough 1990). We use stars with an evolutionary state already determined by Mosser et al. (2012) in order to investigate the characteristics of the glitches as a function of the evolutionary status.

2 Data analysis method

2.1 Data set

Long-cadence data from *Kepler* up to the quarter Q13, corresponding to 1120 days of photometric observation were used. Original light curves were processed and corrected according to the method of García et al. (2011). We used the set of 216 stars for which Mosser et al. (2012) deduced the evolutionary status from the identification of the mixed-mode pattern. This allowed us to select spectra with high signal-to-noise ratio.

2.2 Radial mode fitting method

Pulsating red giant stars are characterized by two distinct resonant cavities, the core and the envelope, giving rise to mixed modes (e.g., Beck et al. 2011; Mosser et al. 2012). These modes behave as acoustic modes in the envelope and as gravity modes in the core. They have a complex frequency pattern. Consequently, we focused on radial modes only. A first estimate of the frequency position of radial modes is determined with the universal pattern (Mosser et al. 2011). This guess is refined by identifying nearby local maxima of the smoothed spectrum with an automated process. We then fit a Lorentzian model to nearby modes with a background component, adjusting the model described by Toutain & Appourchaux (1994), Barban et al. (2010) and Appourchaux (2011).

[1] LESIA, CNRS, Université Pierre et Marie Curie,Université Denis Diderot, Observatoire de Paris, 92195 Meudon cedex, France

2.3 *Determination of the frequency differences* $\Delta\nu(n)$

We calculate the local frequency separation by computing the frequency differences between consecutive radial modes. We derive the local $\Delta\nu(n)$ from the chords between adjacent modes in order to have a central value of the phase:

$$\Delta\nu(n) = \frac{\nu_{n+1,0} - \nu_{n-1,0}}{2}, \tag{2.1}$$

where n is the radial order. At the edges of the measured radial modes, we cannot use Eq. (2.1) and replace it by the frequency difference between two consecutive radial modes.

3 Measuring the glitches for red giants

The difference between the observed local large separation and the asymptotic local large separation predicted by the universal pattern is noted

$$\delta_{\rm g} = \Delta\nu(n) - \Delta\nu_{\rm UP}(n), \tag{3.1}$$

where $\Delta\nu_{\rm UP}(n)$ is the theoretical large separation.

We consider only one oscillatory component in the model used to reproduce $\delta_{\rm g}$ since the discontinuity of the second helium ionisation zone is by far the most important in red giants compared to other discontiniuties as shown by (Miglio et al. 2010). The fitted model is:

$$\delta_{\rm g} = \mathcal{A}\langle\Delta\nu\rangle \cos\left(\frac{2\pi(\nu - \nu_{\max})}{\mathcal{G}\langle\Delta\nu\rangle} + \phi\right), \tag{3.2}$$

where $\langle\Delta\nu\rangle$ is the mean value of the large frequency separation, $\mathcal{G}$ is the period of the oscillation expressed in unit of $\langle\Delta\nu\rangle$, $\mathcal{A}$ is the amplitude of the oscillation in unit of $\langle\Delta\nu\rangle$ and ϕ is the phase of the oscillation centered on $\nu_{\max}$. We used a χ^2 method to fit the three parameters. The uncertainties were extracted by the inversion of the Hessian matrix. In some of the stars we analysed, the performed fit was unsuccessful. This happens for example when the uncertainties on the frequencies are too large. We rejected such fits, when the uncertainties on the period parameter were higher than the measured value of the period.

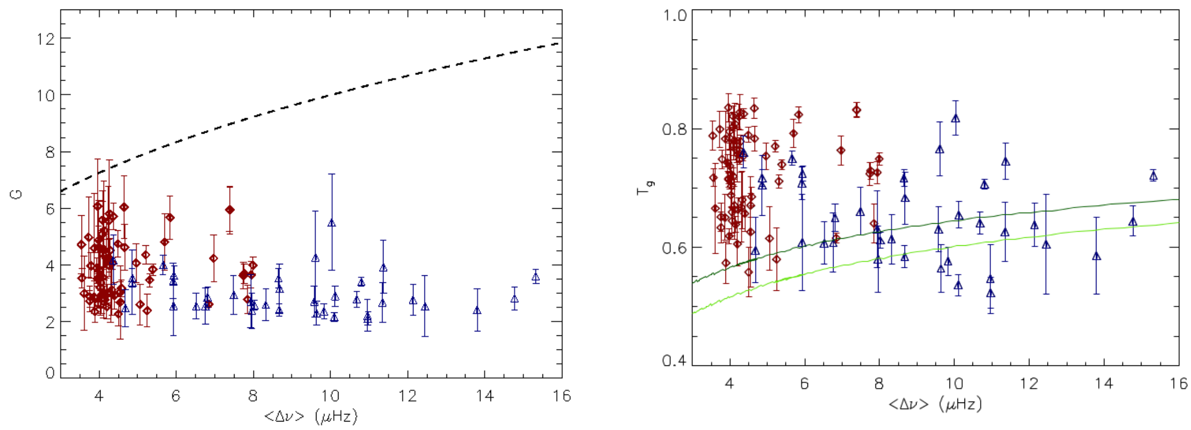

Fig. 1. Left: Dimensionless period $\mathcal{G}$ of the modulation measured as a function of the large separation. Clump stars are indicated by red diamonds and RGB stars by blue triangles. Error bars correspond to the 1σ uncertainties. The dashed black line indicates the maximum number of radial modes observable in a red giant spectrum. **Right:** Acoustic radius of the discontinuity related to the second helium ionisation zone as a function of the global large separation. Clump stars are indicated by red diamonds and RGB stars by blue triangles. Error bars correspond to the 1σ uncertainties. The light green line indicates the theoretical acoustic radius of the second helium ionisation zone for a $1M_\odot$ star during the RGB phase. The dark green line gives the same information for a $1.4M_\odot$ star.

4 Discussion

4.1 Period of the modulation

We measured the dimensionless period $\mathcal{G}$ for 107 stars. The variation of the period as a function of the large separation is shown in Fig. 1. The dimensionless period $\mathcal{G}$ is approximately constant in a large $\langle\Delta\nu\rangle$ range. The mean glitch periods are $\mathcal{G} \simeq 3.88 \pm 0.51$ for clump stars and $\mathcal{G} \simeq 2.85 \pm 0.43$ for RGB stars. Such values are similar to the periods predicted by the models for this kind of star (Broomhall et al. 2014). The period $\mathcal{G}$ is directly related to the acoustic depth of the glitch by the relation (Mazumdar et al. 2014):

$$T_g = \frac{1}{2\langle\Delta\nu\rangle}\left(1 - \frac{1}{2\mathcal{G}}\right). \tag{4.1}$$

The measured T_g are compared to results from models in Fig. 1. The models used are described in Belkacem et al. (2012).

4.2 Phase of the modulation

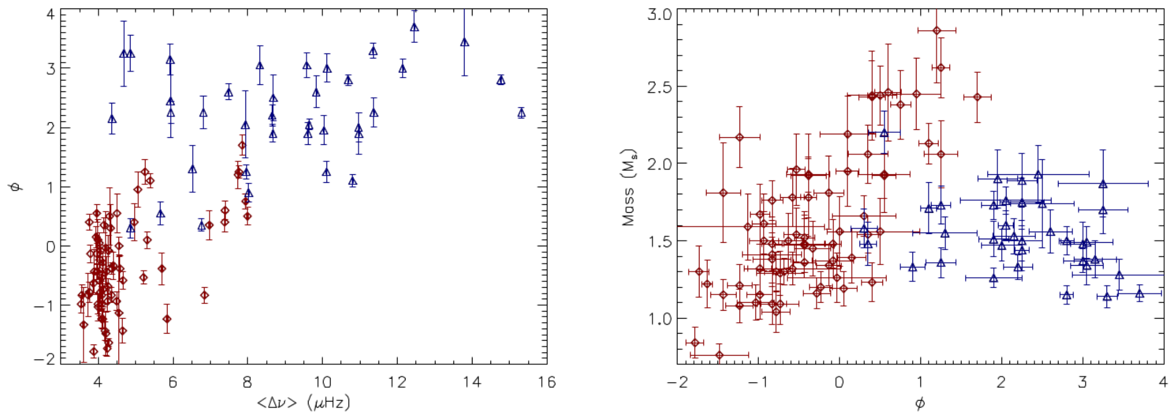

Fig. 2. Left: Phase ϕ of the modulation measured as a function of the global large separation. Clump stars are indicated by red diamonds and RGB stars by blue triangles. Error bars correspond to the 1σ uncertainties. **Right:** Stellar masses in function of the phase of the modulation. Clump stars are indicated by red diamonds and RGB stars by blue triangles. Error bars correspond to the 1σ uncertainties.

The measured phase of the modulation shows complex variation (Fig. 2). All clump stars have a phase around 0, whereas RGB stars have ϕ close to π. This phase shift between clump and RGB stars is systematically observed. To investigate the consequences of this phase difference, we consider the phase at the order corresponding to the index $n_{\max}$ of the maximum oscillation signal. Following Eq. (3.2), if the star has a phase $\simeq 0$ like clump stars, the local large separation measured will be overestimated. On the contrary, if the star has a phase $\simeq \pi$ like RGB stars, the local large separation will be slightly underestimated. This property can be used to determine the evolutionary stage of the stars. The glitch component modifies the local measurement of the large separation with a relative variation of $-0.5\,\%$ for RGB stars and $+1\,\%$ for clump stars. This translate into a change in the ε parameter ($\delta\varepsilon = -(n+\varepsilon)\,\delta\log(\Delta\nu)$), corresponding to $+0.05$ for RGB stars and -0.1 for clump stars. The difference between clump stars and RGB stars is therefore -0.15, in agreement with local measurements (e.g., Bedding et al. 2011; Kallinger et al. 2012). The difference reported by Kallinger et al. (2012) has been noted for a vast majority of red giants. We can therefore conclude that our results, reduced to a limited subset of red giants showing enough oscillation modes, can be extended to all red giants. Therefore, this work justifies the analysis made by Kallinger et al. (2012) for distinguishing RGB and clump stars. Alternatively, measuring the phase shift (Eq. 3.2) provides similar information. Based on the measured $\langle\Delta\nu\rangle$ and $\nu_{\max}$ and on the temperature of the star given by Huber et al. (2013), we deduced the approximate mass and radius of the star from the usual scaling relations (Kallinger et al. 2010; Mosser et al. 2013). We then investigated the mass dependence of the different glitch modulation parameters. Only the phase shows a clear variation with the stellar mass (Fig. 2). Phases of the clump stars have a clear mass dependence: clump stars with a high mass have a higher phase than clump stars with a lower mass. This mass dependence is not seen for RGB stars. The observed relation between the phase and the mass is clear but remains purely empirical. Its physical basis needs to be established.

5 Conclusions

In this work, we have studied the variation of the large separation, $\Delta\nu(n)$, as a function of frequencies for about 200 red giants. For most of the stars, we have found a modulation of $\Delta\nu(n)$ associated to a glitch signature due to the second helium ionisation zone. We have shown that this modulation depends on the evolutionary status of the star which represents a new way to determine the evolutionary stages of red giants. These results have been recently confirmed by theoretical work (Christensen-Dalsgaard et al. 2014).

We acknowledge the entire Kepler team, whose efforts made these results possible. Funding for this Discovery mission was provided by NASA's Science Mission Directorate.

References

Appourchaux, T. 2011, ArXiv e-prints

Barban, C., Baudin, F., Mosser, B., et al. 2010, Astronomische Nachrichten, 331, 1016

Beck, P. G., Bedding, T. R., Mosser, B., et al. 2011, Science, 332, 205

Bedding, T. R., Mosser, B., Huber, D., et al. 2011, Nature, 471, 608

Belkacem, K., Dupret, M. A., Baudin, F., et al. 2012, A&A, 540, L7

Broomhall, A.-M., Miglio, A., Montalbán, J., et al. 2014, MNRAS

Christensen-Dalsgaard, J., Silva Aguirre, V., Elsworth, Y., & Hekker, S. 2014, ArXiv e-prints

García, R. A., Hekker, S., Stello, D., et al. 2011, MNRAS, 414, L6

Gough, D. O. 1990, in Lecture Notes in Physics, Berlin Springer Verlag, Vol. 367, Progress of Seismology of the Sun and Stars, ed. Y. Osaki & H. Shibahashi, 283

Huber, D., Silva Aguirre, V., Matthews, J. M., et al. 2013, ArXiv e-prints

Kallinger, T., Hekker, S., Mosser, B., et al. 2012, A&A, 541, A51

Kallinger, T., Mosser, B., Hekker, S., et al. 2010, A&A, 522, A1

Mazumdar, A., Monteiro, M. J. P. F. G., Ballot, J., et al. 2014, ApJ, 782, 18

Miglio, A., Montalbán, J., Carrier, F., et al. 2010, A&A, 520, L6

Mosser, B., Belkacem, K., Goupil, M., et al. 2011, A&A, 525, L9

Mosser, B., Goupil, M. J., Belkacem, K., et al. 2012, A&A, 540, A143

Mosser, B., Michel, E., Belkacem, K., et al. 2013, A&A, 550, A126

Toutain, T. & Appourchaux, T. 1994, A&A, 289, 649